Energy for Sustainable Development 72 (2023) 326–339

Contents lists available at ScienceDirect

Energy for Sustainable Development

journal homepage: www.journals.elsevier.com/energy-for-sustainable-development

Building envelope-combined phase change material and thermal insulation for energy-effective buildings during harsh summer: Simulation-based analysis

Qudama Al-Yasiri [a,b,c,*], Márta Szabó [b]

[a] Doctoral School of Mechanical Engineering, MATE, Szent István campus, Páter K. u. 1, Gödöllő H-2100, Hungary
[b] Department of Building Engineering and Energetics, Institute of Technology, MATE, Szent István campus, Páter K. u. 1, Gödöllő H-2100, Hungary
[c] Department of Mechanical Engineering, Faculty of Engineering, University of Misan, Al Amarah City, Maysan Province 62001, Iraq

ARTICLE INFO

Keywords:
Phase change material
Thermal insulation
Indoor temperature
Passive building
Thermal comfort
Energy saving

ABSTRACT

Combined phase change material (PCM) and thermal insulation is a crucial practical opportunity to improve thermal inertia and resistance for energy-effective and nearly-zero energy buildings. To this aim, the current paper quantitatively investigated the role of traditional expanded polystyrene (EPS) thermal insulation of different thicknesses to improve the thermal performance of building envelope integrated PCM under harsh summer months. The improvement in indoor temperature was studied considering the maximum indoor temperature reduction (MITR), time lag (TL), average temperature fluctuation reduction (ATFR) and average operative temperature reduction (AOTR). Thereafter, the average heat gain reduction (AHGR) was introduced to quantify the thermal enhancement of envelope elements. Simulation results revealed that building envelope integrated with PCM-EPS demonstrated better thermal performance than incorporating PCM alone. Compared with the PCM room, the indoor temperature of PCM-EPS rooms was improved by a maximum of 143 %, 177.2 %, 35 % and 8.5 % in terms of MITR, TL, ATFR and AOTR, respectively, along with enhanced envelope resistance by up to 103.8 % concerning the AHGR. Increasing EPS layer thickness by up to 2 cm has increased the PCM room thermal performance during the daytime. However, the EPS thickness of 1 cm showed better performance considering the ATFR and AOTR during full thermal cycles.

Introduction

Buildings are the leading sector of global energy consumption and have a high share of CO_2 emissions by up to 36 % and 39 %, respectively (IEA (International Energy Agency), 2018). According to the International Energy Agency and UN Environment Programme, the building envelope is globally responsible for about half of total energy losses, especially in poor insulation buildings (IEA (International Energy Agency) & UN Environment Programme, 2019). Subsequently, high energy-saving opportunities are offered to improve building thermal performance towards nearly-zero energy buildings (NZEBs).

Phase change materials (PCMs) have been publicised lately as a sustainable and effective technique in the building industry due to their significant potential to regulate building envelope thermal energy during the phase change phenomenon (Kharbouch, 2022). Some recent studies have justified the role of PCMs as thermal energy storage in building envelopes to contribute to NZEBs thanks to their high thermal potential for energy management (Li et al., 2022; Stropnik et al., 2019). However, some practical limitations of this technology are still under consideration, mainly related to the seasonal effectiveness of PCMs (Sharaf et al., 2022; Uludaş et al., 2022), stability over the building lifetime (Devanuri et al., 2020; Fabiani et al., 2020), and many others incorporation concerns (Vigna et al., 2018; Zhou et al., 2020). Considering the PCM's influential features, it was reported that increasing PCM thickness generally improves building envelope thermal performance and augments energy-saving (Imafidon & Ting, 2022). However, some drawbacks regarding incomplete solidification/freezing phase in passive applications (Al-Yasiri & Szabó, 2021a), structure mechanical strength weakening (Ren et al., 2021), and economic concerns (M'hamdi et al., 2022; Saafi & Daouas, 2019) have been reported. From another perspective, it has been stated that NZEBs cannot be achieved without installing thermal insulations within buildings (Amani & Kiaee, 2020), which are commonly available and feasible (Gugul et al., 2018). Besides,

* Corresponding author at: Doctoral School of Mechanical Engineering, MATE, Szent István campus, Páter K. u. 1, Gödöllő H-2100, Hungary.
E-mail addresses: qudamaalyasiri@uomisan.edu.iq (Q. Al-Yasiri), szabo.marta@uni-mate.hu (M. Szabó).

https://doi.org/10.1016/j.esd.2023.01.003
Received 25 November 2022; Received in revised form 1 January 2023; Accepted 4 January 2023
Available online 18 January 2023

Nomenclature

Abbreviations

AHGR	Average heat gain reduction [%]
ATFR	Average temperature fluctuation reduction [°C]
AOTR	Average operative temperature reduction [%]
CondFD	Conduction finite difference
DIMS	Dynamic insulation material and system
EPS	Expanded polystyrene
EPW	EnergyPlus weather file
IDF	Information data file
MITR	Maximum indoor temperature reduction [°C]
NZEBs	Nearly-zero energy buildings
OT	Operative temperature [°C]
$OT_{av.,modified}$	Average operative temperature of a modified room with PCM/PCM-EPS [°C]
$OT_{av.,reference}$	Average operative temperature of reference room [°C]
PCM	Phase change material
TIM	Thermal insulation material
TL	Time lag [h]
X	Average decrease of indoor temperature during day hours [°C]
Y	Average increase of indoor temperature during night hours [°C]

Symbols

A	Area [m^2]
C_p	Specific heat capacity [kJ/kg.K]
h	Specific PCM enthalpy [kJ/kg]
h_i	Combined convective and radiative heat transfer coefficient for the interior element surface and interior room temperature [$W/m^2.K$]
h_o	Combined convective and radiative heat transfer coefficient for the outer element surface [$W/m^2.K$]
I_{inc}	Inclined solar radiation intensity on elements [W/m^2]
i	The modelled node
$i+1$	Adjacent node towards indoor zone
i-1	Adjacent node towards outdoor environment
$j+1$	Instant time step [s]
T	Node temperature [K]
T_a	Ambient temperature [K]
$T_{i(av.)modified}$	Average indoor temperature of a modified room with PCM/PCM-EPS [°C]
$T_{i(av.)reference}$	Average indoor temperature of reference room [°C]
T_l	PCM temperature at liquid state [K]
T_s	PCM temperature at the solid state [K]
$T_{sol\text{-}air}$	Solar-air temperature [K]
ΔT	The difference between the interior element surface temperature and indoor temperature [K]
k	Thermal conductivity for PCM at i node [W/m.K]
k_E	Thermal conductivity for the interface between i node and i-1 node [W/m.K]
k_W	Thermal conductivity for the interface between i node and $i+1$ node [W/m.K]
Δt	Time step [s]
Δx	Layer thickness [m]
α	Absorptivity coefficient
ρ	Density [kg/m^3]

installing thermal insulation at adjusted thickness could lessen the importance of PCM, considering the cost of both of them. For instance, Solgi et al. (2019) stated that a combination of 5 mm PCM and 80 mm insulation decreased the cooling load of a wall by 128.3 kJ, compared with 132.4 kJ attained when a combination of 30 mm PCM and 40 mm insulation on the wall.

Numerous studies have investigated the role of insulation in improving the effectiveness of PCM under different climate conditions (Arıcı et al., 2020a; Shahcheraghian et al., 2020; Yu et al., 2020). Amongst others, Jia et al. (2021) numerically studied seven brick walls integrated with different thermal insulation material (TIM) combinations and PCM considering their position within the hollow bricks. The findings commonly displayed that integrating TIM and PCM showed different thermal behaviour in the bricks, in which integrating TIM increased the brick thermal resistance. In contrast, the PCM has improved its thermal inertia. Accordingly, integrating the PCM in the inner side of bricks has reduced the decrement factor from 12.3 %–17.0 % to 1.7 %–2.2 %, enlarged the time lag from 1.5–2 h to 6.2–6.5 h and declined the peak heat flow from 35.2–38.7 W/m^2 to 19.2–26.1 W/m^2. Moreover, the average heat flow increased by 6.1 % when using PCM, while it decreased by 29.7 % when TIM integrated all brick cavities. Nonetheless, integrating TIM-PCM has broadly improved both the thermal resistance and thermal inertia of bricks. Kalbasi and Afrand (2022) conducted a comparative study to explore the best option to reduce the annual energy consumption of walls-integrated insulation, PCM or their combination. PCMs with varied phase transition, namely PCM22 (20 °C-22 °C), PCM23 (21 °C-23 °C) and PCM 24 (22 °C-24 °C), were investigated under Iranian weather of high solar intensity. The findings generally revealed that walls-integrated PCM were better in summer, whereas the insulation performed better in winter. Moreover, the combination of PCM-insulation could lower the total energy demand more than using PCM or insulation alone, in which the use of insulation and PCM24 could reduce the cooling load to zero. However, the study found that the PCM should not exceed 44 % of the total PCM-insulation volume in reducing the annual energy consumption better than applying one of them.

Kishore et al. (2021) proposed a dynamic insulation material and system (DIMS) able to change its thermal resistance based on indoor/outdoor conditions instead of typical insulation with fixed thermal resistance that impacts PCM utilisation. A PCM layer was implanted between two DIMS layers inside the wall arrangement and investigated compared with the wall with PCM only or with DIMS only, under different climate conditions. Numerical findings revealed that the wall integrating PCM-DIMS performed better than with PCM or DIMS only, in which the annual heat gain and heat losses could be reduced by 15 %–72 % and 7 %–38 %, respectively, depending on the climate. Arumugam et al. (2021) analysed the use of PCM, insulation and natural ventilation to enhance the daytime thermal comfort of an office building in India. They considered four building configurations; the first building was set as a reference, the second integrated with PCM, the third integrated insulation and the fourth integrated with both PCM and insulation. Numerical results confirmed that the insulation is suggested when the average nighttime temperature in summer is >27 °C. In contrast, the PCM is recommended when the average nighttime temperature is lower than 27 °C. However, using an air-conditioner at night is required in summer to provide acceptable thermal comfort with natural ventilation during day hours. Besides, the integration of PCM-insulation is suggested for all Indian locations after selecting the suitable PCM/insulation considering the climate conditions. Abden et al. (2022) numerically assessed the total cost saving and increased energy rating of a detached house integrated with PCM gypsum board and expanded polystyrene under three Australian cities, namely Darwin, Alice Springs, and Sydney. The outcomes indicated a total cost saving of AU$167.0, $162.3 and $39.7/$m^2$ was obtained for Darwin, Alice Springs and

Sydney, respectively, at the optimal PCM board-insulation combination over 10 years life cycle. Besides, the house energy ratings increased by 3.5, 3.8 and 4.3 stars in the three cities. Moreover, the renovation payback periods were calculated to be ranged between 2.2 and 7.5 years.

Along with the thermal contribution of the PCM/thermal insulation combination, it is necessary to investigate the mechanical strength of the building structure as well. Several literature studies highlighted that the PCM might decline the strength of the building when incorporated in microcapsules (Alassaad et al., 2021; Lakshan et al., 2021). However, the mechanical properties of building elements could be maintained by incorporating the PCM with suitable percentages (Kontoleon et al., 2021). Besides, integrated PCM within the structure as a layer/panel may avoid mechanical concerns.

Literature studies exhibited notable improvement in the building's thermal performance when integrated with PCM and thermal insulation under moderate weather conditions. These studies have compared the thermal performance of PCM with/without thermal insulation separately (Kalbasi & Afrand, 2022) or considered for specific building elements, mostly walls (Rai, 2021), against limited ones that considered their combination (Abden et al., 2022). The common finding of studies was that the thermal insulation performed superior to PCM, although applying both may attain more benefits based on general analysis and annual operation lifetime. However, there is a lack of studies that consider special cases, such as thin building envelopes, poor thermal construction materials and harsh weather conditions, in which the thermal improvement of using PCM and thermal insulation could be significant.

This work aims to quantify the thermal advantage of installing traditional thermal insulation with PCM-enhanced building envelope under severely hot summer conditions. The optimal position of the thermal insulation with respect to the PCM layer was investigated. Besides, the effect of varying insulation layer thickness (0.5, 1, 1.5 and 2 cm) has been analysed to quantify the advantages considering several indicators of thermal comfort and energy saving over six months. The findings of the current study are trusted to explore the potential of PCM/thermal insulation for improving the built environment, one step towards NZEBs for global sustainable development.

Methodology and construction details

Room model

The current simulations were verified for a stand-alone cubicle room of 100 cm^3 over six consecutive summer months (May–October 2021) for Al Amarah city, Maysan Province (Latitude: 31.84° N and Longitude: 47.14° E) weather conditions. The city is the centre of Misan province, located in the southern part of Iraq, on the border with the Islamic Republic of Iran. The reference room model was built from popular construction materials with poor thermal performance, mainly brick walls and a flat composite roof. The walls were constructed from concrete bricks and an outside cement mortar layer, whereas the composite roof was constructed from Isogam outside roofing layer, concrete layer and gypsum mortar cladding layer. The east wall was provided with a small single-glazing window (35 cm × 25 cm), while a thick plywood foundation was proposed as a floor, matching the real case room investigated in our previous study (Al-Yasiri & Szabó, 2022a). The room was modified with PCM and thermal insulation (with different thicknesses) to investigate thermal performance improvement. Throughout numerical simulations, the floor was considered adiabatic to investigate the role of PCM and insulation into opaque elements (walls and roofs). The room model modified with PCM in the roof and walls is shown in Fig. 1.

Since this work mainly focuses on the impact of insulation on the PCM thermal performance, a single expanded polystyrene (EPS) layer (with different thicknesses) was proposed as a cheap and widely available product for building constructions. Table 1 shows the thermophysical characteristics of construction materials used in the study, as provided in the Iraqi thermal insulation blog for local construction and insulation materials (Ministry of Construction and Housing, 2013).

The PCM employed in the current study is a locally-produced paraffin wax in Iraqi petroleum refineries. It was selected due to its suitability to the variation of temperature in the site under study and favourable thermophysical properties shown in Table 2.

The PCM was integrated into the roof between the Isogam and

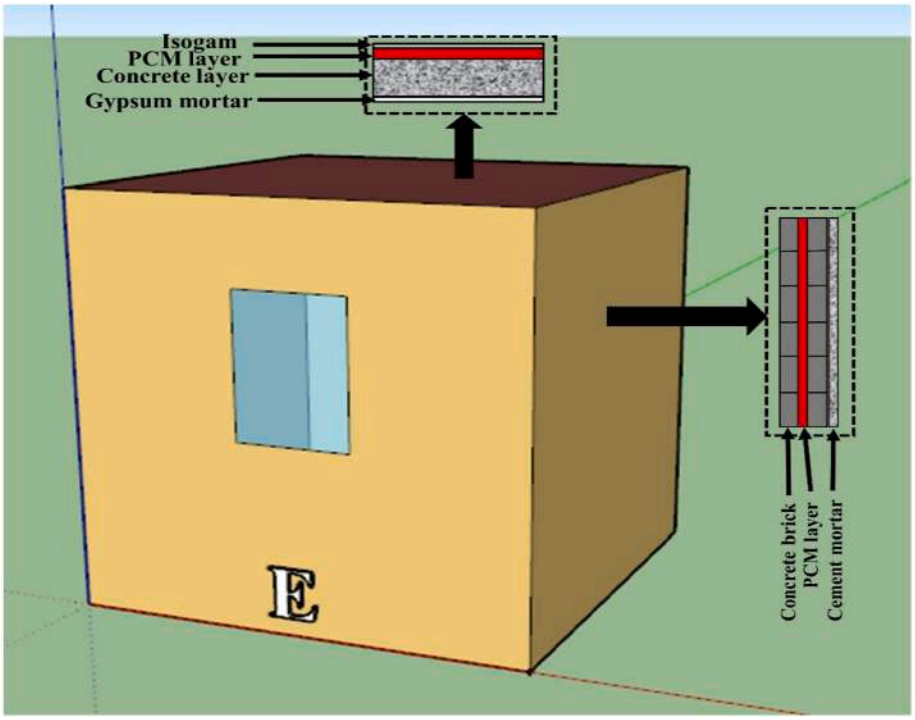

Fig. 1. PCM room model.

Table 1
Thermophysical properties of used construction materials (Gulf insulating material Co. Iraq, 2022; Ministry of Construction and Housing, 2013).

Material	Thickness (cm)	k (W/m.K)	ρ (kg/m^3)	c_p (J/kg.K)
Isogam (roofing layer)	0.4	0.35	1400	1100
Concrete (roof)	5	1.49	2300	800
EPS	0.5, 1, 1.5 and 2	0.035	25	1400
Gypsum mortar (cladding layer for the roof)	0.2	0.23	980	896
Cement mortar (outside layer for walls)	1–2	0.99	2020	1000
Concrete brick (230 × 120) (wall)	7	1.4	1440	750
Plywood (floor)	3	0.18	950	1200
Single pane (U-Factor = 5.48, Solar heat gain coefficient = 0.95)	0.6	–	–	–

Table 2
Thermophysical properties of paraffin wax (PCM) (Akeiber et al., 2016).

Property	Unit	Value
Transition temperature	°C	40–44
Heat of fusion	kJ/kg	190
k (solid/liquid)	W/m.K	0.48/0.22
ρ (solid/liquid)	kg/m^3	830/878
c_p (solid/liquid)	kJ/kg.K	2.21/2.3

concrete roof layers with 1.5 cm thickness, while a layer of 0.7 cm thickness was loaded into the walls at the middle of the bricks. PCM thickness and position in the elements were previously investigated and specified in our experimental studies (Al-Yasiri & Szabó, 2021a; Al-Yasiri & Szabó, 2021b; Al-Yasiri & Szabó, 2021c), considering the PCM thermal performance with the best effectiveness.

Simulation technique

The room model described in Room model subsection was simulated using EnergyPlus software to explore the influence of EPS location and thickness with respect to the PCM layer. The software was developed by the US Department of Energy and widely adopted in building energy simulation studies. The software uses two input files: The energyPlus weather file (EPW) and the information data file (IDF), comprising all required data of the weather and thermophysical characteristics of the building under study. The software provides advanced algorithms for building elements' heat balance and generates heat transfer coefficients and other output variables. The software can simulate buildings-based PCM via a one-dimensional conduction finite-difference (CondFD) solution algorithm to overcome the phase change phenomenon and interactions with the adjacent construction materials. In this regard, the PCM layer loaded into the building envelope is expressed using a fully-implicit first-order scheme shown in Eq. (1) as follows:

$$\rho C_p \Delta x \frac{T_i^{j+1} - T_i^j}{\Delta t} = \left(k_W \frac{\left(T_{i+1}^{j+1} - T_i^{j+1}\right)}{\Delta x} + k_E \frac{\left(T_{i-1}^{j+1} - T_i^{j+1}\right)}{\Delta x} \right) \quad (1)$$

where ρ is the density of the layer (kg/m^3), C_p is the specific heat capacity of the layer (kJ/kg.K), Δx is the thickness of layer (m), and Δt is the time step (s). A Δt of 3 min was used since it is reliable for simulating the PCM phenomenon by EnergyPlus software, following the recommendation of Tabares-Velasco et al. (2012a). T refers to the node temperature (K), whereas i represents the modelled node. Subsequently, $i + 1$ and i-1 represent the neighbouring nodes concerning the inner and outer edges, respectively. $j + 1$ is the immediate time step, whereas j is the last time step. k_W and k_E are the thermal conductivity of the interface between the i and $i + 1$ nodes, and between i and the i-1 nodes, respectively (W/m.K).

The software calculates k_W and k_E by Eq. (2) and Eq. (3), as follows:

$$kw = \frac{\left(k_{i+1}^{j+1} + k_i^{j+1}\right)}{2} \quad (2)$$

$$k_E = \frac{\left(k_{i-1}^{j+1} + k_i^{j+1}\right)}{2} \quad (3)$$

The C_p of the PCM layer is temperature-dependent and calculated by Eq. (4) as follows:

$$C_p = \frac{h_i^j - h_i^{j-1}}{T_i^j - T_i^{j-1}} \quad (4)$$

h is the specific enthalpy of PCM (kJ/kg), defined using the auxiliary function with respect to the PCM temperature as presented in Eq. (5), as follows:

$$h = h(T) \quad (5)$$

The following assumptions were considered to simplify the CondFD algorithm during simulations:

- The PCM and construction materials are homogeneous, isotropic and no heat generation occurs throughout the simulation within the material.
- The PCM, roof and wall layers are in perfect contact with each other (contact resistance is negligible).
- The melting/solidification temperature of the PCM is sharp so that no hysteresis occurs during the simulation.
- The outer surface temperature of the room elements was calculated as a sol-air temperature ($T_{sol\text{-}air}$), based on hourly solar radiation and the outdoor convective heat transfer, according to Eq. (6) (R. and A.-C.E. American Society of Heating, 2016).

$$T_{sol-air} = T_a + \frac{\alpha I_{inc}}{h_o} - 3.9^{\circ}C \text{ for Roof}$$
$$T_{sol-air} = T_a + \frac{\alpha I_{inc}}{h_o} \text{ for walls} \quad (6)$$

where T_a is the ambient temperature (K), α is the element absorptivity coefficient, I_{inc} is the inclined solar radiation on the element (W/m^2), and h_o is the convective-radiative heat transfer coefficient of outer element surfaces (W/m^2.K).

Model verification

Many researchers have validated the building models carried out using EnergyPlus software in the literature against experimental and numerical studies (Sharma & Rai, 2020; Tabares-Velasco et al., 2012b). The results of the established model in the current study were validated with our previous experimental study, which examined full-scale rooms using the same construction materials and climate conditions (Al-Yasiri & Szabó, 2022a). The model simulation results in terms of indoor temperature for the room with/without PCM were compared with the experimental study results and were in good agreement in both the reference and PCM rooms, as shown in Fig. 2. The maximum deviation reported between the numerical and experimental findings were 6.1 % and 7.9 % in the reference and PCM rooms, respectively. The result deviation is mainly attributed to the slight deviation of weather data between the in-site measurements in the experimental study and those provided in the EPW file in the simulation. Moreover, the thermophysical properties of the materials delivered in the software's IDF file were not exactly as the room construction materials used in the experimental study since they were adopted from the standard insulation blog (Ministry of Construction and Housing, 2013).

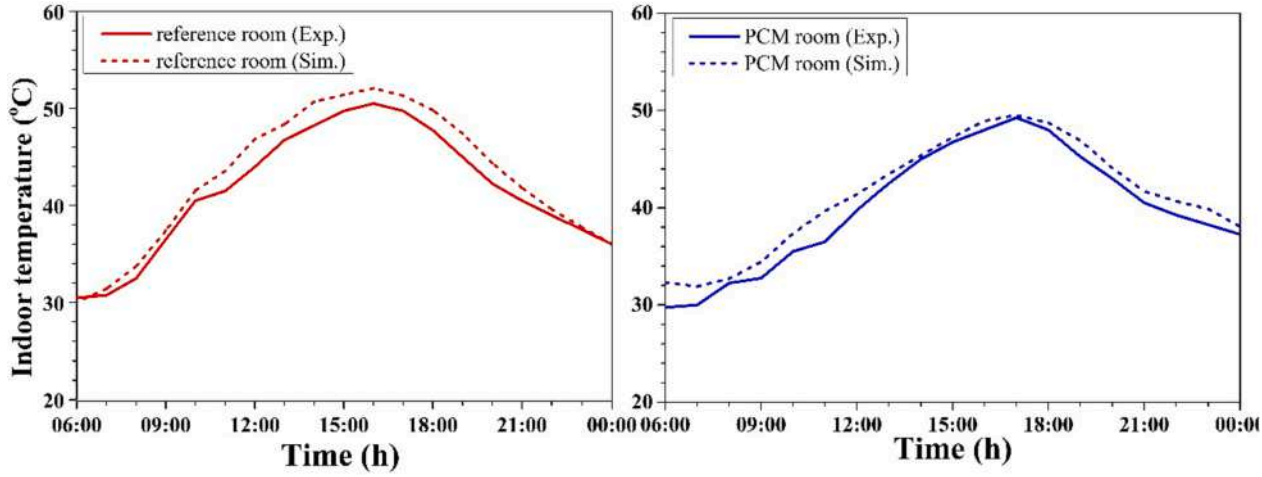

Fig. 2. Verification of the EnergyPlus model (indoor temperature of reference and PCM rooms) (Al-Yasiri & Szabó, 2022a).

Assessment of PCM/PCM-EPS room thermal performance

The performance of the proposed rooms was assessed considering the zone indoor temperature variation and total average heat gain. In this regard, some concepts were studied to quantify and analyse the impact of the EPS insulation and PCM on the room's thermal performance. These concepts are the maximum indoor temperature reduction, time lag, average operative temperature reduction, average temperature fluctuation reduction and total average heat gain reduction.

At first, the role of EPS insulation was determined by specifying the best influential position with respect to the PCM layer within the roof since it has many layers and highly influences the room performance (Al-Yasiri & Szabó, 2022b). Later, the best position of the EPS layer is adopted to investigate the PCM room thermal performance when several EPS thicknesses are installed in the roof and walls. To this aim, a simulation was conducted on a composite roof involving 1 cm of EPS in three different positions for a specific day in July. During simulations, the walls and floor of the room were set as adiabatic, while the roof (described in Room model subsection) contained an additional EPS layer placed in different positions (shown in Fig. 3), as follows:

a) Between the Isogam and PCM layers (termed as "*EPS-o*", indicating the EPS position near the outdoor environment),
b) Between the PCM and concrete layers (termed as "*EPS-m*", indicating the EPS position in the middle of the roof composition), and
c) Between the concrete and gypsum mortar layers (termed as "*EPS-i*", indicating the EPS position near the indoor zone).

The best position of the EPS layer was identified by determining the position with minimal influence on the PCM effectiveness in terms of its liquid fraction as the best variable to monitor PCM effectiveness (Arıcı et al., 2020b). In other words, the best EPS layer position is considered the position with the lowest influence on the PCM melting and solidification to avoid a negative impact on the PCM phase change during the thermal cycle. The liquid fraction denotes the amount of liquid PCM out of the total PCM amount (liquid and solid), ranging from 0 to 1, in which the value 0 means no liquid PCM found, whereas the value 1 means the PCM is fully melted. Mathematically, the liquid fraction is calculated according to Eq. (7) as follows:

$$\textit{Liquid fraction} = \begin{cases} 0 & \text{if } T_n \geq T_l \text{ (Solid phase)} \\ \dfrac{T - T_s}{T_l - T_s} & \text{if } T_l > T \geq T_s \text{ (Mushy zone)} \\ 1 & \text{if } T_n < T_s \text{(Melting phase)} \end{cases} \quad (7)$$

where T represents the node temperature within the PCM layer. T_l and T_s are the PCM temperatures at the liquid and solid states (i.e., melting and solidification phases).

Results and discussion

Study location

The simulation in the current study was confirmed for Al Amarah city, Maysan Province, southern Iraq (shown in Fig. 4), over six summer months, May–October 2021. This location is dominated by the hot summer season, classified as a desert climate according to the Köppen Geiger climate classification (Köppen climate classification, 2022). July is the hottest summer month which usually has long sunshine hours and high ambient temperatures, typically exceeding 45 °C during the day and 30 °C at night. On the other side, October represents the transition month characterised by relatively high diurnal temperatures and cold nights.

Averagely, Fig. 5 shows the outdoor air bulb temperature (outdoor temperature) of the location under study during the simulated period.

The solar radiation rate falling on the room (i.e., walls and roof) is essential to determine the outside element surface temperature and heat transfer coefficients. Fig. 6 shows the average hourly solar radiation on building elements during the simulated period. As observed in the figure, the roof was exposed to a high solar radiation rate for a long time

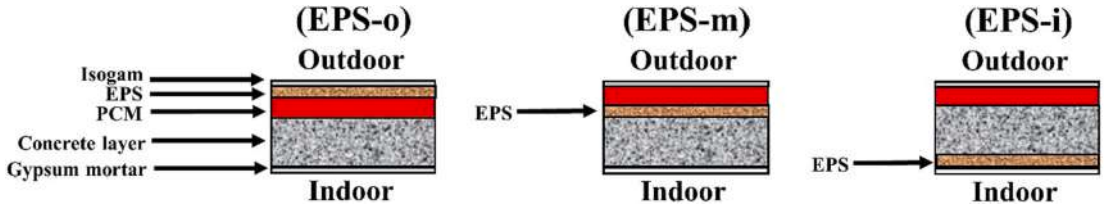

Fig. 3. EPS position cases in the roof combination.

Fig. 4. Study location (Al Amarah city).

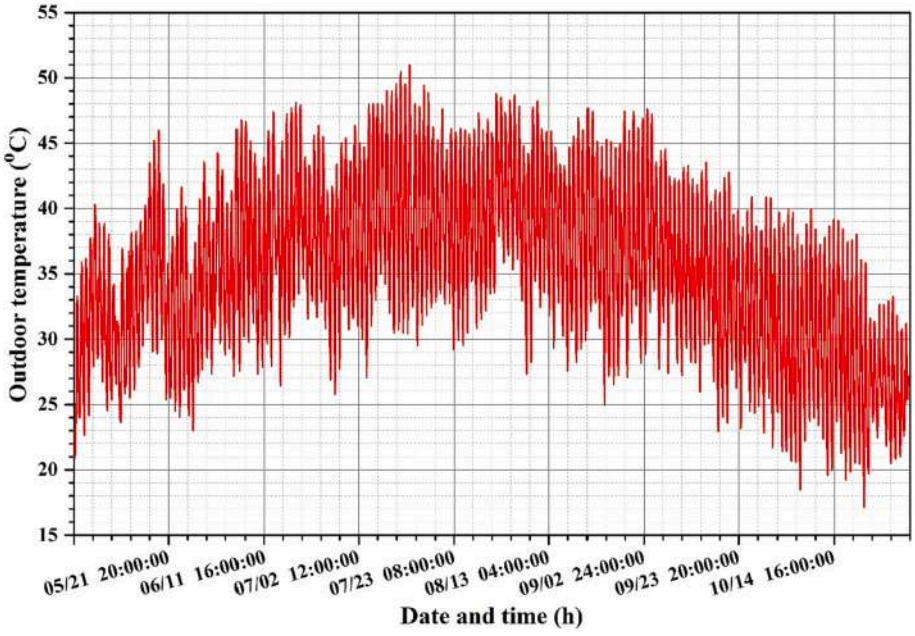

Fig. 5. Average hourly outdoor temperature during the simulated period.

a day, from 9:00 to 16:00, exceeding 1000 W/m^2 in June, July and August. Besides, the solar radiation rates on the east and west walls were higher than that on the north and south walls, showing about 700–800 W/m^2 in the above summer months. However, October shows a different trend of solar radiation where the east wall showed higher rates than the roof, and the south wall received more radiation than in previous months.

The variation of outdoor ambient temperature and solar radiation primarily stimulates the PCM in the current work since the simulation was carried out under no ventilation. Consequently, the heat transfer phenomenon through the building envelope was controlled by changeable outdoor conditions during the thermal cycle.

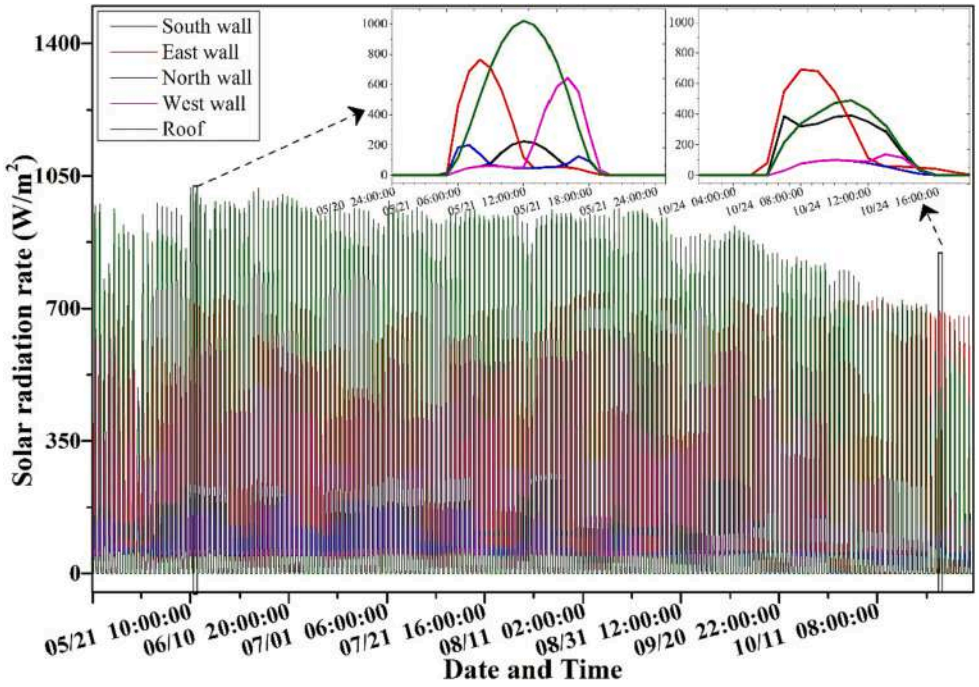

Fig. 6. Solar radiation of the site under study during 2021.

Analysis of the optimal insulation position

As indicated in Assessment of PCM/PCM-EPS room thermal performance subsection, the EPS layer was placed in different positions to investigate the best position with the lowest effect on the PCM activation considering the PCM liquid fraction. To reach this aim, a simulation was verified for the three proposed EPS positions within a roof construction (highlighted in Fig. 3) on the 21st of July, the typical summer design day in the thermal calculations made under Iraqi weather conditions (Al-Mudhafar et al., 2021; Mustafa et al., 2020). The simulation results in terms of the liquid fraction of the PCM layer in each case (i.e., EPS-I, EPS-m and EPS-o) are shown in Fig. 7.

On the whole, the cases where the EPS layer was placed near the indoor environment (i.e., EPS-i and EPS-m) showed better PCM liquid fraction evolution than the case where the EPS layer was placed outside (i.e., EPS-o). The PCM started the melting phase at 9:00 with about 0.08 melting fraction in the case of EPS-m, while it was in a solidification phase in the EPS-i and EPS-o. At 10:00, the PCM was partially melted in all cases, reaching 0.54, 0.61 and 0.41 in the EPS-i, EPS-m and EPS-o, respectively. The PCM was in a liquid state (i.e., melting fraction equal to 1) at 11:00 in the EPS-i and EPS-m cases, while it was partially melted with a liquid fraction of 0.92 in the EPS-o case.

The PCM was in a liquid state at 12:00–18:00 in all cases, indicating no influence of the EPS layer on the PCM in this period. However, the

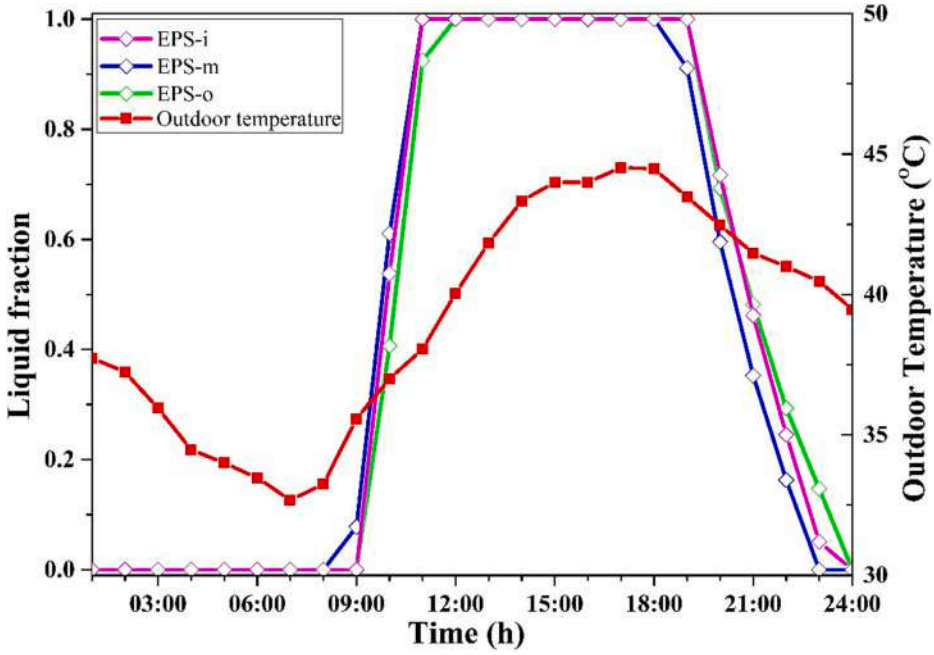

Fig. 7. Liquid fraction of PCM layer within roof combination.

PCM solidified at 19:00 in the EPS-m case with 0.91 liquid fraction, whereas the PCM was in a liquid state in the EPS-i and EPS-o cases. The PCM was partially melted from 20:00 till 22:00 with better solidification in the case of EPS-m followed by EPS-i and then EPS-o. Later, the PCM layer was fully solidified at 23:00 in the case of EPS-m, while it was partially solidified in the case of EPS-i and EPS-o with a liquid fraction of 0.05 and 0.15, respectively. At 12:00, the PCM was in a solid phase in all cases, indicating the suitability of the high PCM melting temperature (40–44 °C) with the temperature level at night even though the PCM was involved passively within the roof structure.

The above analysis shows that the PCM was activated better when placed after the EPS layer towards the outdoor environment, and the best EPS position is in the middle of the roof construction. This is logical since the outdoor ambient temperature is the main controller of PCM melting and solidification in passive PCM applications. Besides, the insulation layer will decrease the temperature necessary for PCM activation, which impacts the melting and solidification phases. Besides, installing the insulation layer near the outside environment would affect the phase change of PCM; thus, it should be incorporated towards the inside with a lower melting temperature (Rai, 2021). Based on the above analysis, the EPS layer will be positioned directly after the PCM layer towards the indoor environment (i.e., in the EPS-m case) to investigate the role of the EPS layer with different thicknesses, namely 0.5, 1, 1.5 and 2 cm, on the PCM room thermal performance.

Analysis of indoor temperature at different insulation thicknesses

Literature studies have confirmed the potential of PCM to shave and shift the indoor peak temperature if properly incorporated with the building envelope (Al-Absi et al., 2022; Tunçbilek et al., 2020). Besides, thermal insulations could improve the thermal resistance of buildings, minimising heat transfer towards the indoor environment. However, installing thermal insulation could maximise the benefits of PCM since the thermal insulation increases the building's thermal resistance, whereas the PCM improves the building's thermal inertia (Jia et al., 2021). This combination of PCM/thermal insulation is critical in severe hot location buildings where the PCM has limited effectiveness when reaching full melting early. In contrast, increasing PCM quantity could cause economic worries and negative behaviour during solidification.

Thermal insulation thickness could impact PCM's effectiveness since the phase transition associated with the temperature variation across the PCM layer and increasing the insulation thickness may reduce the temperature below the necessary phase change level. Therefore, the optimal thermal insulation thickness should be specified to ensure the

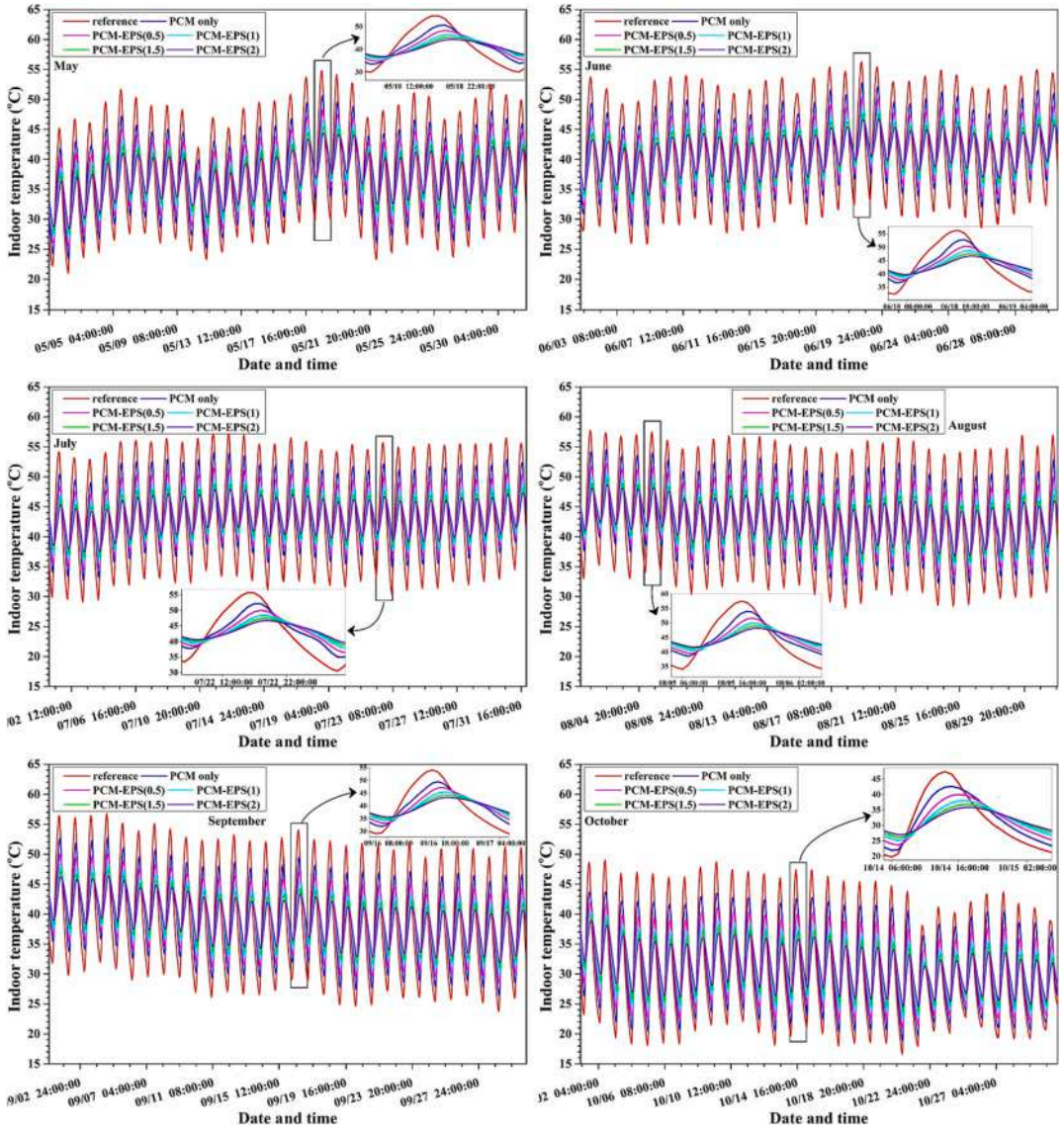

Fig. 8. Hourly indoor temperature variation in each month (May–October).

effective use of PCM and promote the thermal storage benefits.

This section investigates the advances in indoor air temperature when different thermal insulation (EPS) thicknesses are installed in a PCM room, placed directly after the PCM layer near the indoors. The simulation performed for the room with PCM only and PCM combined with EPS of 0.5, 1, 1.5 and 2 cm thicknesses, termed as PCM-EPS(0.5), PCM-EPS(1), PCM-EPS(1.5) and PCM-EPS(2), respectively. The indoor temperature variation of studied cases each month is shown in Fig. 8.

According to Fig. 8, the increased EPS layer thickness has reduced the indoor temperature and shaved the maximum temperature at midday hours. This behaviour is expected since increasing the envelope thickness (of any material) usually reduces the heat transfer rate and indoor temperature due to increased envelope resistance, according to Fourier's law (Garrido et al., 2001). However, the indoor temperature showed reversed behaviour during night hours in which the thicker EPS layer caused worsen performance than the thinner one since the indoor space was not ventilated. Therefore, the accumulated heat took a long time to transfer towards the outdoor. Thus, the indoor temperature behaviour and its correlation with the PCM activation during the thermal cycle should be evaluated well to indicate the best EPS thickness. Consequently, the following subsections briefly discuss several indicators to show indoor temperature behaviour: maximum indoor reduction, time lag, average temperature fluctuation reduction, and average operative temperature reduction.

Maximum indoor temperature difference

The maximum indoor temperature reduction (MITR) refers to the reduction in the maximum indoor temperature of the modified room (with PCM and PCM-EPS) compared with the reference room. This indicator was calculated as the temperature difference between the maximum indoor temperature in each modified room with that of the reference room considering the monthly hottest day, specifically May 19th, June 18th, July 12th, August 1st, September 4th and October 2nd. The MITR results are shown in Fig. 9.

In general, the MITR trend was relatively similar in all months, even though the temperature variation during the day was different (e.g., July the hottest and October the coldest month). This is because the MITR calculations considered the hottest day monthly, which were relatively similar, exceeding 45 °C. However, this figure could provide a reasonable indication of the building's ability to cope with heat waves and increase in ambient temperature in the future as globally expected due to climate change (Liu et al., 2021). It is obvious in Fig. 9 that the indoor temperature decreased as the insulation thickness increased, resulting from the improved envelope's thermal resistance against outdoor heat flow. Amongst months, May exhibited lowest MITR by about 3.8 °C, 5.5 °C, 7.1 °C, 8.1 °C and 8.9 °C respectively in the PCM, PCM-EPS(0.5), PCM-EPS(1), PCM-EPS(1.5) and PCM-EPS(2) rooms, whereas September showed the highest by 4.3 °C, 6.6 °C, 8.4 °C, 9.6 °C and 10.4 °C, respectively.

On average for all months, the room with PCM showed MITR of 3.9 °C compared with the reference room, against 6.1 °C, 7.6 °C, 8.7 °C and 9.5 °C in the PCM-EPS(0.5), PCM-EPS(1), PCM-EPS(1.5) and PCM-EPS(2) cases, respectively. Conclusively, installing an EPS layer of increased thickness by 0.5 cm with the PCM room has reduced the MITR by a ratio of 55.7 %, 95.4 %, 123.1 % and 142.8 %, respectively, compared with incorporating PCM only.

Time lag

The time lag (TL) generally refers to the daily time delay of peak (maximum) indoor temperature compared with the peak outdoor temperature, representing an essential indicator of building envelope thermal resistance. This indicator and the MITR provide a crucial indication of building envelope physical performance to stabilise indoor temperature and contribute mostly to NZEBs (Rathore et al., 2020). The TL in this study was calculated as the average daily time delay difference between the peak indoor temperature of the modified room (with PCM only or with PCM-EPS) in comparison with that of the reference room. This indicator was calculated in minutes since the TL would be similar in some months with hourly calculations, resulting imprecise evaluation of the PCM room with different EPS thicknesses. The calculation results of TL are presented in Fig. 10.

All modified rooms showed remarkable TL compared with the reference room. Nevertheless, incorporating PCM into the room showed lower TL than PCM-EPS cases. Moreover, the thicker EPS layer installed in the PCM room has extended the TL due to increased room thermal resistance. In this regard, the PCM room showed maximum TL by about

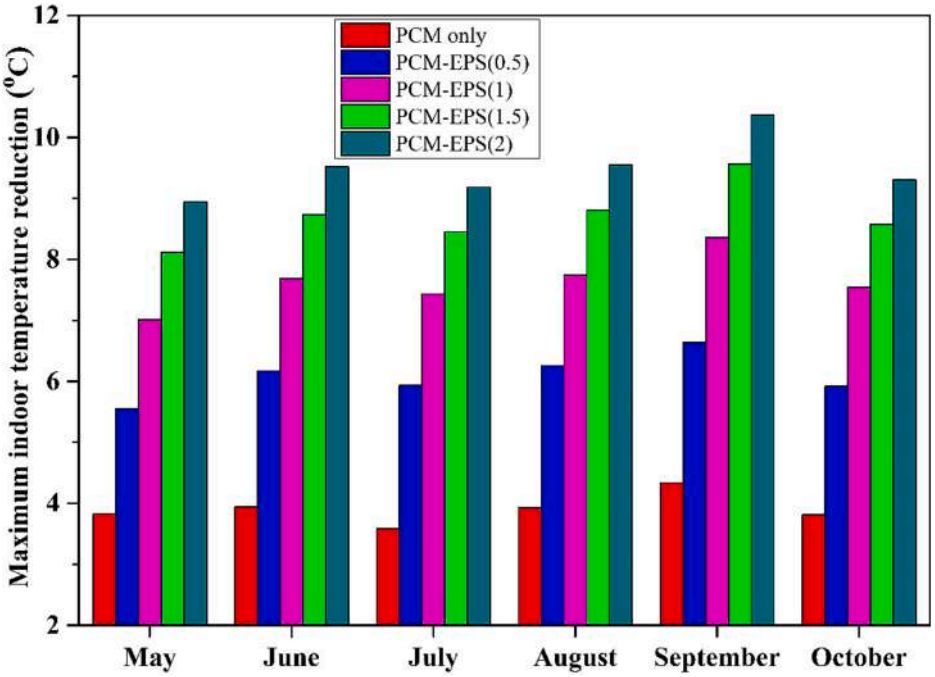

Fig. 9. MITR of PCM/PCM-EPS rooms against the reference room.

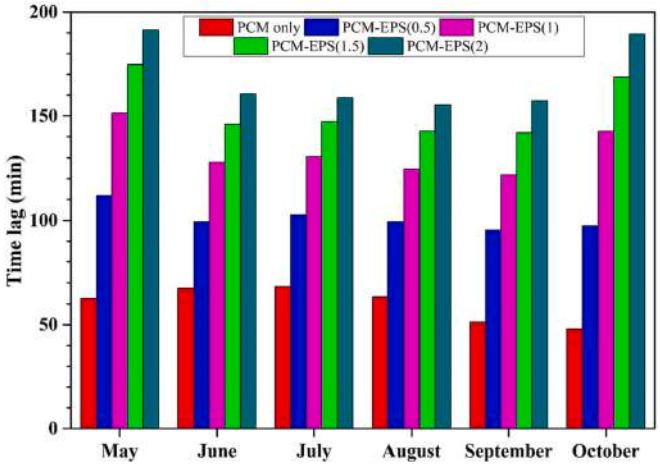

Fig. 10. TL of modified rooms compared with the reference room.

1 h compared with 1.9 h for the PCM-EPS(0.5), 2.5 h for PCM-EPS(1), 2.9 h for the PCM-EPS(1.5) and 3.2 h for the PCM-EPS(2) during the simulation period. Considering all months, the TL in May was longer than in other months, except October, whereas September showed a shorter TL. Besides, the PCM room showed better TL during June and July against poor TL in September and October. These results are associated with the peak diurnal temperature and PCM effectiveness each month in which the higher outdoor temperatures had shown priority for PCM incorporation compared with the reference room. Therefore, October indicated lower utilisation of PCM, which was working as an additional insulation layer with no thermal storage potential.

On average of the simulated period, the PCM room displayed TL by an average of ~1 h compared with the reference room against 1.7 h, 2.2 h, 2.6 h and 2.8 h in the PCM-EPS(0.5), PCM-EPS(1), PCM-EPS(1.5) and PCM-EPS(2) rooms, respectively. These results are equivalent to an extended TL period in the PCM room by 68.3 %, 117.8 %, 157.4 % and 177.2 % when installing an extra EPS layer of 0.5, 1, 1.5 and 2 mm, respectively.

Average temperature fluctuation reduction

Considering the thermal behaviour of PCM and its impact on the daily indoor temperature is necessary to determine the best thermal insulation thickness and ensure the PCM's full melting/solidification cycle. The average indoor temperature fluctuation reduction (ATFR) refers to the reduction of indoor temperature fluctuations in the modified room in comparison with the reference room throughout the day cycle. The ATFR is usually calculated considering the indoor temperature variation of the complete thermal cycle to consider the positive thermal performance (average indoor temperature reduction) in the modified room during day time and the negative thermal performance of the modified room during nighttime (Kenzhekhanov et al., 2020). Therefore, the ATFR value is estimated in this work by summing the average indoor temperature reduction in the modified room with respect to the reference one from 6:00 to 18:00 (called X) plus the adverse indoor temperature behaviour of the modified room compared with the reference room during the night from 18:00 to 24:00 (called as Y). Accordingly, ATFR>0 °C indicates a positive enhancement in the indoor temperature and vice versa when ATFR<0 °C, whereas no enhancement is achieved if ATFR = 0. Accordingly, monthly ATFR was quantified by Eq. (8), concerning X as the day and Y as the night period, as indicated in Eqs. (9) and (10).

$$\mathrm{ATFR} = \mathrm{X} + \mathrm{Y} \tag{8}$$

$$\mathrm{X} = \mathrm{T}_{i(av.),reference} - \mathrm{T}_{i(av.),modified} \tag{9}$$

$$\mathrm{Y} = \mathrm{T}_{i(av.),modified} - \mathrm{T}_{i(av.),reference} \tag{10}$$

where $T_{i(av.),reference}$ and $T_{i(av.),modified}$ are respectively the average indoor temperature in the reference and modified rooms (°C). Fig. 11 presents the average ATFR values during each simulated month.

The ATFR results presented in Fig. 11 indicated crucial thermal behaviour of the simulated room under different thermal insulation thicknesses. The ATFR outcomes exhibited different behaviour than the MITR and TL that were discussed lastly. The ATFR was relatively similar in May–September, then totally different in October. In May–September, the PCM-EPS(1) displayed the highest ATFR, followed by PCM-EPS(0.5) compared with the PCM-EPS(1.5) and PCM-EPS(2) cases. The average ATFR during simulated months was 4.6 °C, 6.1 °C, 6.2 °C, 5.9 °C and 5.5 °C respectively in the PCM room, PCM-EPS(0.5), PCM-EPS(1), PCM-EPS(1.5) and PCM-EPS(2) rooms. Equivalently, these values represent an enhancement in the indoor temperature during the day cycle in the PCM room by 32.9 %, 35.4 %, 28.4 % and 19.8 % when adding EPS layers with 0.5, 1, 1.5 and 2 cm thickness. This is because the EPS restricts the indoor heat dissipation towards outdoor ambient due to EPS' low thermal conductivity, keeping the indoor zone at a high temperature for a long time during the night. This thermal behaviour will worsen as the EPS layer thickness increases. Although the PCM-EPS(1) room has higher EPS thickness than the PCM-EPS(0.5) room, the average indoor temperature of the PCM-EPS(1) room compared with the reference room during day time (i.e., X) was higher than that of the PCM-EPS(0.5). This was against a slight difference in the nighttime (i.e., Y) between PCM-EPS(0.5) and PCM-EPS(1), resulting in a better ATFR for the PCM-EPS (1) throughout the thermal cycle.

The thermal performance of ATFR was different in October, as indicated in Fig. 11, in which the thicker EPS layer incorporated with the PCM room resulted in better ATFR. This is attributed to the fact that the PCM did not activate well during most of October due to low outdoor ambient temperature; hence, the PCM layer behaved as a traditional construction layer with low thermal conductivity. Besides, the outdoor ambient temperature in October was low enough to accelerate heat dissipation from inside the thermal zone towards outside, regardless of EPS thickness, resulting in low Y values against high X values of increased EPS thickness. The latter reason confirms the ATFR results during July, for instance, which showed the worsening behaviour due to high outdoor ambient temperature at night that influenced the heat transfer rate between the indoor and outdoor environments, which eventually negatively impacted the rooms with thicker EPS layers.

Average operative temperature reduction

Thermal comfort has little devotion in the literature when researchers investigate the combined use of PCM and thermal insulations, focussing more on energy-saving aspects in terms of cooling and heating loads (Vautherot et al., 2015). Consequently, the average operative temperature reduction (AOTR) is discussed in this section as an essential thermal comfort indicator. The operative temperature (OT) stands for the temperature sensed inside the built environment by residents, resulting from the average indoor air and mean radiant surface temperature (calculated by the EnergyPlus software) of the interior envelope (ANSI/ASHRAE Standard 55-2010, 2010). The AOTR is calculated in the current study considering the average indoor temperature of modified rooms (with PCM and with PCM-EPS) compared with the reference room from 6:00 to 18:00. Mathematically, the AOTR was calculated using Eq. (11), as follows:

$$AOTR = \frac{OT_{av.,reference} - OT_{av.,modified}}{OT_{av.,reference}} \times 100\% \tag{11}$$

The calculation results of the AOTR of the simulated rooms can be shown in Fig. 12.

Fig. 12 indicates better AOTR for the modified rooms than the reference room, with superior behaviour for PCM-EPS over the PCM

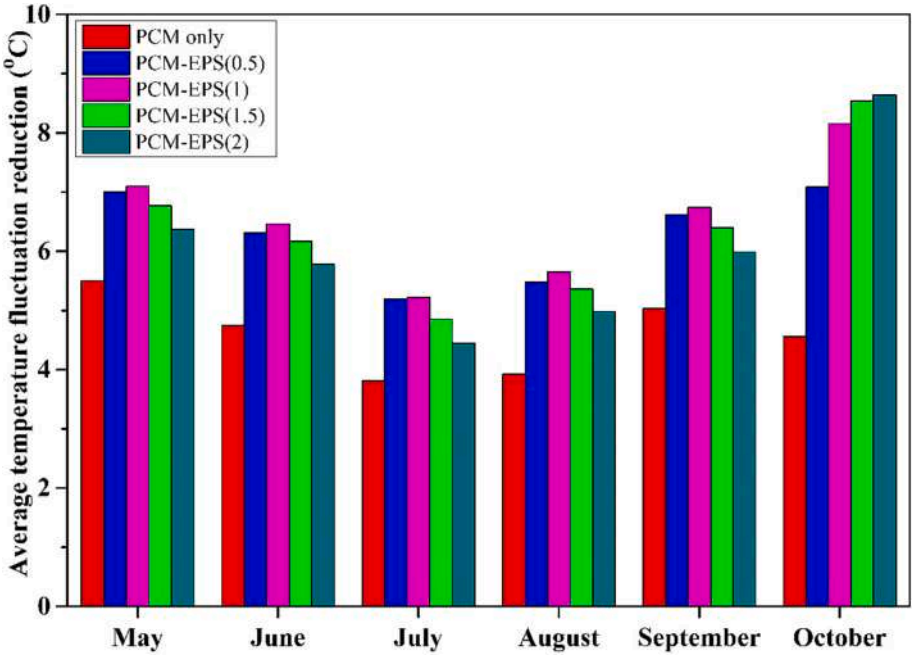

Fig. 11. ATFR of modified rooms compared with the reference room.

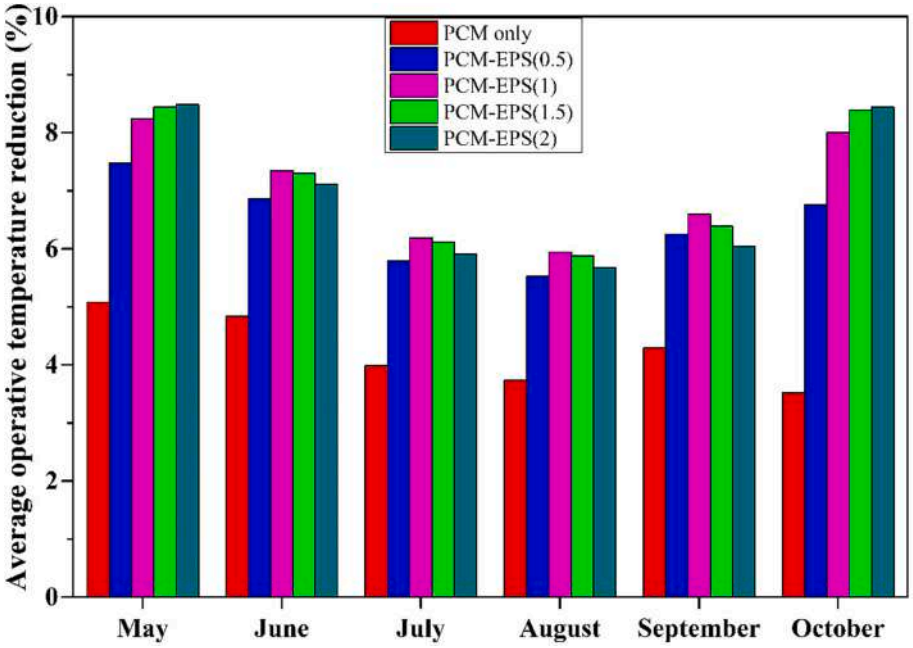

Fig. 12. AOTR of modified rooms compared with the reference room.

layer during the simulation months. The rooms integrated with EPS showed different enhancement trends in which the thicker EPS layer performed better during May and October. In contrast, the EPS with 1 cm thickness showed better behaviour during June–September. The AOTR in May and October was around 4.3 %, 7.1 %, 8.1 %, 8.4 % and 8.5 % for the room with PCM, PCM-EPS(0.5), PCM-EPS(1), PCM-EPS (1.5) and PCM-EPS(2), respectively. In contrast, the average AOTR in June–September was 4.2 %, 6.3 %, 6.6 %, 6.4 % and 6.1 % for the mentioned cases, respectively. This diverse trend could be attributed to the nighttime outdoor temperature level. In this regard, May and October had lower outdoor ambient temperatures than the other months (June–September), leading to full solidification of PCM and complete dissipation of indoor heat before the next thermal cycle. Therefore, the AOTR associated with the average decrease in room indoor and interior surface temperature was better for the PCM-EPS of higher thickness.

In contrast, the relatively high outdoor ambient temperature during the nights of June–September had delayed the heat dissipation from the indoor zone of thicker EPS cases, resulting in poor AOTR in the following thermal cycle. This can be noticed from the negative OT difference between the modified and reference rooms at the beginning day hours (around 6:00 till 8:00) of June–September, due to poor heat dissipation at night in the room with thick EPS. In conclusion, the EPS with 0.5 and 1 cm thickness were suitable for installation with the PCM to keep the zone OT within acceptable level during June–September more than EPS

with 1.5 and 2 cm thickness. Besides, the thicker EPS layer installed in the PCM room could improve indoor OT during low outdoor temperatures.

Analysis of envelope thermal performance

Analysing the thermal performance of building elements is vital to quantify the energy-saving owing to installing the thermal insulation with PCM, especially for the current case, since it focuses on building envelope enhancement regardless of other cooling load sources (lighting, equipment, appliances, etc.). The solar heat gain resulting from envelope elements is the best indicator to calculate the thermal improvement in this study, dealing mainly with the inside surface temperature of envelope elements (the roof and walls).

The solar heat gain across the room could be estimated according to Eq. (12) (Al-Rashed et al., 2021) considering the combined convective/radiative heat transfer coefficient of elements (h_i, W/m^2.K), element area (m^2), and the difference of interior element surface temperature and indoor air temperature (K).

$$Heat\ gain = h_i\, A \Delta T \tag{12}$$

Since the current study focuses on the role of thermal insulation when combined with a PCM room, the total average heat gain reduction (AHGR) was calculated for the PCM-EPS room cases compared with the PCM room. The AHGR is quantified by considering the heat gain difference between each element in the PCM-EPS room compared with the corresponding elements of the PCM room during the day hours. Consequently, the AHGR of PCM-EPS rooms was estimated according to Eq. (13) as follows:

$$\mathrm{AHGR} = \frac{HG_{av.,PCM} - HG_{av.,PCM-EPS}}{HG_{av.,PCM}} \times 100\% \tag{13}$$

Fig. 13 presents the AHGR of each PCM-EPS case over simulated months.

As observed in Fig. 13, the AHGR increased as the insulation layer thickness increased compared to the PCM layer. On average, the AHGR was increased by 51.1 %, 80.9 %, 95.1 %, and 103.8 %, respectively, when EPS layer of 0.5, 1, 1.5 and 2 cm thickness was installed in the PCM room. This is evident since the HG of the envelope element is dependent on the thermal resistance of element layers (i.e., R-value), which is specified by the layer's thermal conductivity and thickness (Holman, 2011). The AHGR varied during the simulation months, showing the lowest values in July against the higher ones in October. Incidentally, increasing EPS layer thickness by 0.5 cm over the PCM-EPS (0.5) has increased the AHGR by about 50.5 %, 74.5 % and 86.1 % in July, in contrast to 71.2 %, 114.4 % and 135.2 %, respectively in October. The reason is that the PCM was more effective in July due to phase change phenomena, which lessened the importance of EPS layer thickness increment in the PCM-EPS cases compared with the case of PCM only. In contrast, the PCM was useless during October and acted as a traditional construction material of fixed thermal conductivity (i.e., no phase change phenomena). Therefore, increasing EPS layer thickness has augmented the thermal resistance of the envelope compared with the element with PCM only, as stated previously by Solgi et al. (2019).

Insights for future work

The outcomes of the current study underlined the advantages of combining thermal insulation with PCM to the building thermal comfort and energy saving under non-conditioned zone. However, the thermal performance of PCM and its effect on the indoor temperature could be different in other conditions, such as using night air ventilation and/or space air conditioning systems. These cases could be investigated in the future for further improvement of indoor thermal comfort and better thermal performance of PCM towards nearly-zero energy and energy-efficient buildings. Some other insights could be adopted in future studies, as follows:

- The environmental and economic analysis could be applied to provide a complete vision of the technology. The environmental aspect could be overcome by considering the energy saving of HVAC systems in real case study buildings integrated with PCM and thermal insulation against a reference case building. At the same time, the static payback period indicator could be adopted to quantify the feasibility of incorporating PCM/thermal insulation over the building service lifetime.
- It is worth highlighting that installing the EPS layer may influence the usefulness of PCM during winter since it affects solar radiation

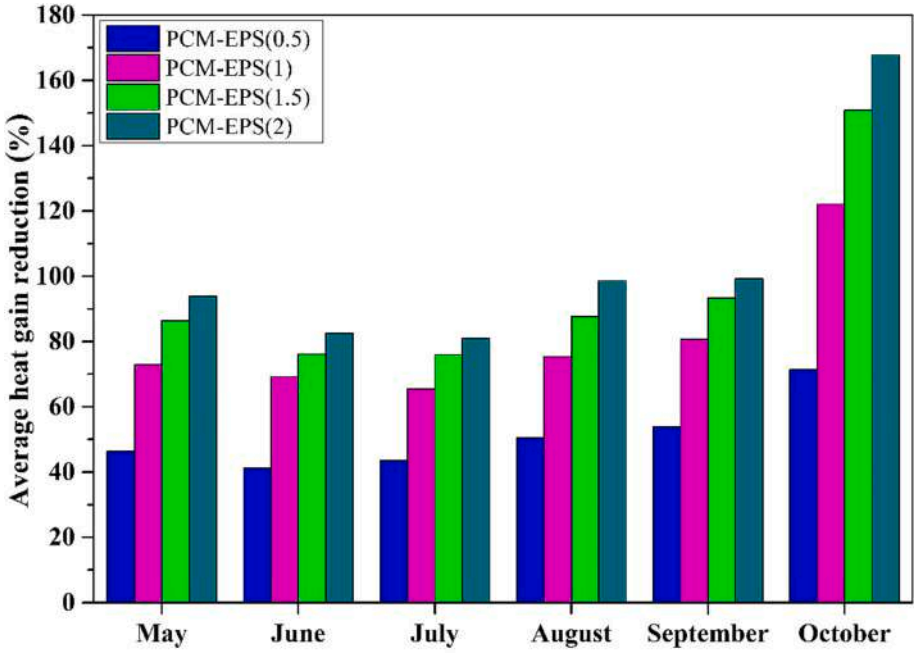

Fig. 13. AHGR of PCM-EPS rooms compared with the PCM room.

utilisation. The optimal position attained in the current study could be assumed effective even during winter since it was located on the inside edge of the PCM layer. Nevertheless, the optimal thickness in such cases should be specified properly, along with selecting the optimal PCM melting range. This research scope is still beyond deep investigation, even though some literature studies revealed that active PCM is superior to passive incorporation in winter to employ solar energy for heating load reduction (Kong et al., 2020).

- The sustainability behind using the PCM/thermal insulation combination could be discussed in future studies along with the thermal and energy contribution in line with the latest report of the United Nations Environment Programme and the International Energy Agency (United Nations, 2021).

Conclusion

The current work investigated the combined use of PCM and thermal insulation to improve the building's thermal performance and support the measures towards nearly-zero energy buildings. The conclusions from the current study findings include:

- In general, increasing the EPS layer thickness installed on the PCM room has improved the room performance considering daytime, whereas the improvement is limited when considering the whole thermal cycle. Moreover, the following conclusions can be drawn from the current study:
- The PCM performance is highly influenced by increasing thermal insulation thickness when incorporated passively into the building structure with no ventilation.
- Regarding the optimal position of thermal insulation, installing the EPS layer directly after the PCM layer from the indoor side guarantees efficient melting and solidification phases in terms of PCM liquid fraction. The PCM started melting phase one hour earlier at this position than when positioning the EPS layer near the indoor or outdoor environments and reached full solidification before the end of the day.
- The indoor temperature in terms of MITR was improved with the same percentage during the simulated months as the EPS layer thickness increased. Incidentally, the average monthly increase of MITR reached 55.7 %, 95.4 %, 123.1 % and 142.8 % when the EPS layer thickness increased by 0.5, 1, 1.5 and 2 cm, respectively, over the PCM room.
- Increasing EPS layer thickness in the PCM room extends the TL due to increased envelope thermal resistance, reaching up to 3 h and 12 min over the reference room.
- According to ATFR analysis during May–September, installing an EPS layer with 1 cm thickness into the PCM room had attained maximum ATFR by about 35 %, compared with only 20 % when a 2 cm EPS layer thickness was installed. However, this behaviour was different in October. The thicker EPS layer installed with the PCM room performed better due to increased envelope thermal resistance under non-activated PCM and low outdoor ambient temperature.
- The AOTR is associated with the outdoor ambient temperature at night in which a thicker EPS layer than 1 cm performed poorly compared with that of an EPS layer thickness equal to/or lower than 1 cm during June–September. In contrast, the thicker EPS layer installed with the PCM room showed better AOTR by up to 8.5 % during May and October.
- Increased insulation layer thickness generally increases the AHGR of envelope elements. However, the increment ratio associated with the effectiveness of PCM in which increased insulation thickness benefits in July was much lower than in October.
- Overall, the thermal advantages attained from integrated thermal insulation with the PCM room notably impact the environmental and economic viewpoints.

Declaration of competing interest

The authors declare that they have no known competing financial interests or personal relationships that could have appeared to influence the work reported in this paper.

Acknowledgements

This work was supported by the Stipendium Hungaricum Scholarship Programme and the Doctoral School of Mechanical Engineering, MATE-Szent István campus, Gödöllő, Hungary. The first author would like to acknowledge Dr. Aakash Rai from Birla Institute of Technology and Science, India, for his valuable directions in conducting the simulations.

References

Abden, M. J., Tao, Z., Alim, M. A., Pan, Z., George, L., & Wuhrer, R. (2022). Combined use of phase change material and thermal insulation to improve energy efficiency of residential buildings. *Journal of Energy Storage., 56*, Article 105880. https://doi.org/10.1016/j.est.2022.105880

Akeiber, H. J., Wahid, M. A., Hussen, H. M., & Mohammad, A. T. (2016). A newly composed paraffin encapsulated prototype roof structure for efficient thermal management in hot climate. *Energy, 104*, 99–106. https://doi.org/10.1016/j.energy.2016.03.131

Al-Absi, Z. A., Hafizal, M. I. M., & Ismail, M. (2022). Experimental study on the thermal performance of PCM-based panels developed for exterior finishes of building walls. *Journal of Building Engineering, 52*, Article 104379. https://doi.org/10.1016/j.jobe.2022.104379

Alassaad, F., Touati, K., Levacher, D., & Sebaibi, N. (2021). Impact of phase change materials on lightened earth hygroscopic, thermal and mechanical properties. *Journal of Building Engineering., 41*, Article 102417. https://doi.org/10.1016/j.jobe.2021.102417

Al-Mudhafar, A. H. N., Hamzah, M. T., & Tarish, A. L. (2021). Potential of integrating PCMs in residential building envelope to reduce cooling energy consumption. *Case Studies in Thermal Engineering, 27*, Article 101360. https://doi.org/10.1016/j.csite.2021.101360

Al-Rashed, A. A. A. A., Alnaqi, A. A., & Alsarraf, J. (2021). Energy-saving of building envelope using passive PCM technique: a case study of Kuwait City climate conditions. *Sustainable Energy Technologies and Assessments, 46*, Article 101254. https://doi.org/10.1016/j.seta.2021.101254

Al-Yasiri, Q., & Szabó, M. (2021). Case study on the optimal thickness of phase change material incorporated composite roof under hot climate conditions. *Case Stud. Constr. Mater., 14*, Article e00522. https://doi.org/10.1016/j.cscm.2021.e00522

Al-Yasiri, Q., & Szabó, M. (2021). Experimental evaluation of the optimal position of a macroencapsulated phase change material incorporated composite roof under hot climate conditions. *Sustainable Energy Technologies and Assessments, 45*, Article 101121. https://doi.org/10.1016/j.seta.2021.101121

Al-Yasiri, Q., & Szabó, M. (2021). Thermal performance of concrete bricks based phase change material encapsulated by various aluminium containers: an experimental study under Iraqi hot climate conditions. *Journal of Energy Storage, 40*, Article 102710. https://doi.org/10.1016/j.est.2021.102710

Al-Yasiri, Q., & Szabó, M. (2022). Energetic and thermal comfort assessment of phase change material passively incorporated building envelope in severe hot climate: an experimental study. *Applied Energy, 314*, Article 118957. https://doi.org/10.1016/j.apenergy.2022.118957

Al-Yasiri, Q., & Szabó, M. (2022). Phase change material coupled building envelope for thermal comfort and energy-saving: effect of natural night ventilation under hot climate. *Journal of Cleaner Production, 365*, Article 132839. https://doi.org/10.1016/j.jclepro.2022.132839

Amani, N., & Kiaee, E. (2020). Developing a two-criteria framework to rank thermal insulation materials in nearly zero energy buildings using multi-objective optimization approach. *Journal of Cleaner Production, 276*, Article 122592. https://doi.org/10.1016/j.jclepro.2020.122592

ANSI/ASHRAE Standard 55-2010. (2010). Thermal environmental conditions for human occupancy. In *Encycl. Financ.*. https://doi.org/10.1007/0-387-26336-5_1680

Arıcı, M., Bilgin, F., Nižetić, S., & Karabay, H. (2020). PCM integrated to external building walls: An optimization study on maximum activation of latent heat. *Applied Thermal Engineering, 165*, Article 114560. https://doi.org/10.1016/j.applthermaleng.2019.114560

Arıcı, M., Tütüncü, E., Yıldız, Ç., & Li, D. (2020). Enhancement of PCM melting rate via internal fin and nanoparticles. *International Journal of Heat and Mass Transfer, 156*, Article 119845. https://doi.org/10.1016/j.ijheatmasstransfer.2020.119845

Arumugam, P., Vellaichamy, P., Ramalingam, V., Prakash, S. Arun, & V., A. A. R. (2021). A pathway towards healthy and naturally ventilated indoor built environment through phase change material and insulation techniques for office buildings in India. *Proc. Inst. Mech. Eng. Part A J. Power Energy, 236*, 555–574. https://doi.org/10.1177/09576509211056426

Devanuri, J. K., Gaddala, U. M., & Kumar, V. (2020). Investigation on compatibility and thermal reliability of phase change materials for low-temperature thermal energy

storage. *Mater. Renew. SustainEnergy, 9*, 1–16. https://doi.org/10.1007/s40243-020-00184-4

Fabiani, C., Pisello, A. L., Barbanera, M., & Cabeza, L. F. (2020). Palm oil-based bio-PCM for energy efficient building applications: Multipurpose thermal investigation and life cycle assessment. *Journal of Energy Storage., 28*, Article 101129. https://doi.org/10.1016/j.est.2019.101129

Garrido, P. L., Hurtado, P. I., & Nadrowski, B. (2001). Simple One-Dimensional Model of Heat Conduction which Obeys Fourier's Law. *Physical Review Letters, 86*, 5486–5489. https://doi.org/10.1103/PhysRevLett.86.5486

Gugul, G. N., Aydinalp Koksal, M., & Ugursal, V. I. (2018). Techno-economical analysis of building envelope and renewable energy technology retrofits to single family homes. *energySustainable Development, 45*, 159–170. https://doi.org/10.1016/j.esd.2018.06.006

Gulf insulating material Co. Iraq. (2022). http://www.newiraqnet.net/com/1/gulf/gulf_e.htm.

Holman, J. P. (2011). *Heat transfer* (10th ed.). INDIA: MC GRAW HILL https://www.academia.edu/36379481/Heat_Transfer_Tenth_Edition_Jack_P_Holman_.

IEA (International Energy Agency). (2018). *The future of cooling: opportunities for energy-efficient air conditioning*. https://pronto-core-cdn.prontomarketing.com/449/wp-content/uploads/sites/2/2018/06/Melanie-Slade-The-Future-of-Cooling-Opportunities-for-Energy-Efficient-Air-Conditioning.pdf.

IEA (International Energy Agency), UN Environment Programme. (2019). *2019 global status report for buildings and construction: Towards a zero-emission, efficient and resilient buildings and construction sector*. https://www.worldgbc.org/news-media/2019-global-status-report-buildings-and-construction.

Imafidon, O. J., & Ting, D. S.-K. (2022). Energy consumption of a building with phase change material walls – the effect of phase change material properties. *Journal of Energy Storage., 52*, Article 105080. https://doi.org/10.1016/j.est.2022.105080

Jia, C., Geng, X., Liu, F., & Gao, Y. (2021). Thermal behavior improvement of hollow sintered bricks integrated with both thermal insulation material (TIM) and Phase-Change Material (PCM). *Case Studies in Thermal Engineering, 25*, Article 100938. https://doi.org/10.1016/j.csite.2021.100938

Kalbasi, R., & Afrand, M. (2022). Which one is more effective to add to building envelope: phase change material, thermal insulation, or their combination to meet zero-carbon-ready buildings? *Journal of Cleaner Production, 367*, Article 133032. https://doi.org/10.1016/j.jclepro.2022.133032

Kenzhekhanov, S., Memon, S. A., & Adilkhanova, I. (2020). Quantitative evaluation of thermal performance and energy saving potential of the building integrated with PCM in a subarctic climate. *Energy, 192*, Article 116607. https://doi.org/10.1016/j.energy.2019.116607

Kharbouch, Y. (2022). Effectiveness of phase change material in improving the summer thermal performance of an office building under future climate conditions: an investigation study for the Moroccan Mediterranean climate zone. *Journal of Energy Storage., 54*, Article 105253. https://doi.org/10.1016/j.est.2022.105253

Kishore, R. A., Bianchi, M. V. A., Booten, C., Vidal, J., & Jackson, R. (2021). Enhancing building energy performance by effectively using phase change material and dynamic insulation in walls. *Applied Energy, 283*, Article 116306. https://doi.org/10.1016/j.apenergy.2020.116306

Kong, X., Wang, L., Li, H., Yuan, G., & Yao, C. (2020). Experimental study on a novel hybrid system of active composite PCM wall and solar thermal system for clean heating supply in winter. *Solar Energy, 195*, 259–270. https://doi.org/10.1016/j.solener.2019.11.081

Kontoleon, K. J., Stefanidou, M., Saboor, S., Mazzeo, D., Karaoulis, A., Zegginis, D., & Kraniotis, D. (2021). Defensive behaviour of building envelopes in terms of mechanical and thermal responsiveness by incorporating PCMs in cement mortar layers. *Sustainable Energy Technologies and Assessments, 47*, Article 101349. https://doi.org/10.1016/j.seta.2021.101349

Köppen climate classification. (2022). https://www.weatherbase.com/weather/weather-summary.php3?s=56604&cityname=Al+Amarah%2C+Maysan%2C+Iraq&units=.

Lakshan, R. R., Rosini, A. M., Sathiyan, K., Gangadharan, D., Sathyan, D., & Mini, K. M. (2021). Study on thermal insulating properties of PCM incorporated wall panels. *Materials Today: Proceedings, 46*, 5118–5122. https://doi.org/10.1016/j.matpr.2020.10.501

Li, H., Li, Y., Wang, Z., Shao, S., Deng, G., Xue, H., Xu, Z., & Yang, Y. (2022). Integrated building envelope performance evaluation method towards nearly zero energy buildings based on operation data. *Energy and Buildings, 268*, Article 112219. https://doi.org/10.1016/j.enbuild.2022.112219

Liu, T., Zhou, C., Zhang, H., Huang, B., Xu, Y., Lin, L., Wang, L., Hu, R., Hou, Z., Xiao, Y., Li, J., Xu, X., Jin, D., Qin, M., Zhao, Q., Gong, W., Yin, P., Xu, Y., Hu, J., … Ma, W. (2021). Ambient Temperature and years of Life lost: A national study in China. *Innovation, 2*, Article 100072. https://doi.org/10.1016/j.xinn.2020.100072

M'hamdi, Y., Baba, K., Tajayouti, M., & Nounah, A. (2022). Energy, environmental, and economic analysis of different buildings envelope integrated with phase change materials in different climates. *Solar Energy, 243*, 91–102. https://doi.org/10.1016/j.solener.2022.07.031

Ministry of Construction and Housing. (2013). *Ministry of Planning,Thermal Insulation Blog (Iraqi Construction Blog)*. ttps://amanatbaghdad.gov.iq/amanarules/pict/مدونات/blog20-مدونة العزل الحراري.pdf.

Mustafa, M., Ali, S., Snape, J. R., & Vand, B. (2020). Investigations towards lower cooling load in a typical residential building in Kurdistan (Iraq). *Energy Reports., 6*, 571–580. https://doi.org/10.1016/j.egyr.2020.11.011

R. and A.-C.E. American Society of Heating. (2016). *2016 ASHRAE Handbook-HVAC Systems and Equipment* (IP ed.). ASHRAE.

Rai, A. C. (2021). Energy performance of phase change materials integrated into brick masonry walls for cooling load management in residential buildings. *Building and Environment, 199*, Article 107930. https://doi.org/10.1016/j.buildenv.2021.107930

Rathore, P. K. S., Shukla, S. K., & Gupta, N. K. (2020). Yearly analysis of peak temperature, thermal amplitude, time lag and decrement factor of a building envelope in tropical climate. *Journal of Building Engineering, 31*, Article 101459. https://doi.org/10.1016/j.jobe.2020.101459

Ren, M., Wen, X., Gao, X., & Liu, Y. (2021). Thermal and mechanical properties of ultra-high performance concrete incorporated with microencapsulated phase change material. *Construction and Building Materials, 273*, Article 121714. https://doi.org/10.1016/j.conbuildmat.2020.121714

Saafi, K., & Daouas, N. (2019). Energy and cost efficiency of phase change materials integrated in building envelopes under Tunisia Mediterranean climate. *Energy, 187*, Article 115987. https://doi.org/10.1016/j.energy.2019.115987

Shahcheraghian, A., Ahmadi, R., & Malekpour, A. (2020). Utilising latent thermal energy storage in building envelopes to minimise thermal loads and enhance comfort. *Journal of Energy Storage., 33*, Article 102119. https://doi.org/10.1016/j.est.2020.102119

Sharaf, M., Yousef, M. S., & Huzayyin, A. S. (2022). Year-round energy and exergy performance investigation of a photovoltaic panel coupled with metal foam/phase change material composite. *Renewable Energy, 189*, 777–789. https://doi.org/10.1016/j.renene.2022.03.071

Sharma, V., & Rai, A. C. (2020). Performance assessment of residential building envelopes enhanced with phase change materials. *Energy and Buildings, 208*, Article 109664. https://doi.org/10.1016/j.enbuild.2019.109664

Solgi, E., Hamedani, Z., Fernando, R., & Mohammad Kari, B. (2019). A parametric study of phase change material characteristics when coupled with thermal insulation for different Australian climatic zones. *Building and Environment, 163*, Article 106317. https://doi.org/10.1016/j.buildenv.2019.106317

Stropnik, R., Koželj, R., Zavrl, E., & Stritih, U. (2019). Improved thermal energy storage for nearly zero energy buildings with PCM integration. *Solar Energy, 190*, 420–426. https://doi.org/10.1016/j.solener.2019.08.041

Tabares-Velasco, P. C., Christensen, C., & Bianchi, M. (2012). Verification and validation of EnergyPlus phase change material model for opaque wall assemblies. *Building and Environment, 54*, 186–196. https://doi.org/10.1016/j.buildenv.2012.02.019

Tabares-Velasco, P. C., Christensen, C., Bianchi, M., & Booten, C. (2012). *Verification and validation of EnergyPlus conduction finite difference and phase change material models for opaque wall assemblies*. Golden, CO (United States): National Renewable Energy Lab.(NREL).

Tunçbilek, E., Arıcı, M., Bouadila, S., & Wonorahardjo, S. (2020). Seasonal and annual performance analysis of PCM-integrated building brick under the climatic conditions of Marmara region. *Journal of Thermal Analysis and Calorimetry, 141*, 613–624. https://doi.org/10.1007/s10973-020-09320-8

Uludaş, M.Ç., Tunçbilek, E., Yıldız, Ç., Arıcı, M., Li, D., & Krajčík, M. (2022). PCM-enhanced sunspace for energy efficiency and CO2 mitigation in a house in mediterranean climate. *Journal of Building Engineering, 57*, Article 104856. https://doi.org/10.1016/j.jobe.2022.104856

United Nations. (2021). *2021Global Status Report for Buildings and Construction: Towards a Zero-emissions, Efficientand Resilient Buildings and Construction Sector*. https://globalabc.org/resources/publications/2021-global-status-report-buildings-and-construction.

Vautherot, M., Maréchal, F., & Farid, M. M. (2015). Analysis of energy requirements versus comfort levels for the integration of phase change materials in buildings. *Journal of Building Engineering, 1*, 53–62. https://doi.org/10.1016/j.jobe.2015.03.003

Vigna, I., Bianco, L., Goia, F., & Serra, V. (2018). Phase change materials in transparent building envelopes: a Strengths, weakness, Opportunities and Threats (SWOT) analysis. *Energies, 11*. https://doi.org/10.3390/en11010111

Yu, J., Leng, K., Ye, H., Xu, X., Luo, Y., Wang, J., Yang, X., Yang, Q., & Gang, W. (2020). Study on thermal insulation characteristics and optimized design of pipe-embedded ventilation roof with outer-layer shape-stabilized PCM in different climate zones. *Renewable Energy, 147*, 1609–1622. https://doi.org/10.1016/j.renene.2019.09.115

Zhou, Y., Zheng, S., Liu, Z., Wen, T., Ding, Z., Yan, J., & Zhang, G. (2020). Passive and active phase change materials integrated building energy systems with advanced machine-learning based climate-adaptive designs, intelligent operations, uncertainty-based analysis and optimisations: a state-of-the-art review. *Renewable and Sustainable Energy Reviews, 130*, Article 109889. https://doi.org/10.1016/j.rser.2020.109889